J. Geogr. Sci. 2019, 29(2): 253-270
DOI: https://doi.org/10.1007/s11442-019-1595-0

Spatio-temporal evolution and the influencing factors of $PM_{2.5}$ in China between 2000 and 2015

ZHOU Liang[1,2], ZHOU Chenghu[2], YANG Fan[3], CHE Lei[4], WANG Bo[5], *SUN Dongqi[2]

1. Faculty of Geomatics, Lanzhou Jiaotong University, Lanzhou 730070, China;
2. Institute of Geographic Sciences and Natural Resources Research, CAS, Beijing 100101, China;
3. School of Geographic and Oceanographic Sciences, Nanjing University, Nanjing 210023, China;
4. College of Geography and Environment Sciences, Northwest Normal University, Lanzhou 730070, China;
5. Department of Geography, The University of Hong Kong, Hong Kong 999077, China

Abstract: High concentrations of $PM_{2.5}$ are universally considered as a main cause for haze formation. Therefore, it is important to identify the spatial heterogeneity and influencing factors of $PM_{2.5}$ concentrations for regional air quality control and management. In this study, $PM_{2.5}$ data from 2000 to 2015 was determined from an inversion of NASA atmospheric remote sensing images. Using geo-statistics, geographic detectors, and geo-spatial analysis methods, the spatio-temporal evolution patterns and driving factors of $PM_{2.5}$ concentration in China were evaluated. The main results are as follows. (1) In general, the average concentration of $PM_{2.5}$ in China increased quickly and reached its peak value in 2006; subsequently, concentrations remained between 21.84 and 35.08 μg/m^3. (2) $PM_{2.5}$ is strikingly heterogeneous in China, with higher concentrations in the north and east than in the south and west. In particular, areas with relatively high $PM_{2.5}$ concentrations are primarily in four regions, the Huang-Huai-Hai Plain, Lower Yangtze River Delta Plain, Sichuan Basin, and Taklimakan Desert. Among them, Beijing-Tianjin-Hebei Region has the highest concentration of $PM_{2.5}$. (3) The center of gravity of $PM_{2.5}$ has generally moved northeastward, which indicates an increasingly serious haze in eastern China. High-value $PM_{2.5}$ concentrations have moved eastward, while low-value $PM_{2.5}$ has moved westward. (4) Spatial autocorrelation analysis indicates a significantly positive spatial correlation. The "High-High" $PM_{2.5}$ agglomeration areas are distributed in the Huang-Huai-Hai Plain, Fenhe-Weihe River Basin, Sichuan Basin, and Jianghan Plain regions. The "Low-Low" $PM_{2.5}$ agglomeration areas include Inner Mongolia and Heilongjiang, north of the Great Wall, Qinghai-Tibet Plateau, and Taiwan, Hainan, and Fujian and other southeast coastal cities and islands. (5) Geographic detection analysis indicates that both natural and anthropogenic factors account for spatial variations in $PM_{2.5}$ concentration. Geographical location, population density, automobile quantity, industrial discharge, and straw burning are the main driving forces of $PM_{2.5}$ concentration in China.

Received: 2018-05-10 **Accepted:** 2018-10-22
Foundation: The Strategic Priority Research Program of the Chinese Academy of Sciences, No.XDA19040401; China Postdoctoral Science Foundation, No.2016M600121; National Natural Science Foundation of China, No.41701173, No.41501137; The State Key Laboratory of Resources and Environmental Information System
Author: Zhou Liang, PhD and Associate Professor, specialized in environmental geography, urban geography and regional development. E-mail: zhougeo@126.com
***Corresponding author:** Sun Dongqi, Associate Professor, specialized in urban geography. E-mail: sundq@igsnrr.ac.cn

Keywords: air pollution; $PM_{2.5}$; haze; spatio-temporal evolution; environmental influence; China

1 Introduction

$PM_{2.5}$ is the most serious air pollutant in China, which shows typical regional and compound pollution characteristics. Concurrently with rapid urbanization and industrialization in China, energy consumption and car ownership have increased sharply. The airborne dust caused by urbanization, atmospheric pollution caused by coal burning, and emissions from automobile exhaust fumes have become more serious, which have led to a dramatic increase in total suspended particles (TSP) in the air (Hueglina *et al*., 2005; Stone, 2008; Huang, 2018). Haze has become increasingly frequent year after year, forming four geographic haze areas: the Huang-Huai-Hai Region, Yangtze River Delta, Sichuan Basin, and Pearl River Delta (Guo *et al*., 2011; Wu, 2012). China's successive promulgation of a series of environmental protection laws and rules, long-term atmospheric prevention and control measures, and industrial and energy structural adjustment and upgrading during "the 11th Five-Year Plan" in 2006–2010 and "the 12th Five-Year Plan" in 2011–2015 have resulted in a distinct reduction in SO_2, SO_x, and dust. However, it is widely recognized that $PM_{2.5}$ (particulate matter with an aerodynamic diameter no greater than 2.5 μm) has become a striking challenge for China's atmospheric pollution prevention and control. $PM_{2.5}$ is closely related to human activities inside the atmospheric boundary layer. $PM_{2.5}$ lowers visibility and participates in chemical reactions in the atmosphere to generate new pollutants and severely affects human health. Medical studies have shown that $PM_{2.5}$ enters the human respiratory system, which can result in various respiratory and cardiovascular diseases, an attenuation of lung function, destruction of the human immune system, and possible increases in risk of death in the exposed population (Dockery *et al*., 1994; Pope *et al*., 1995; Laden *et al*., 2000; Pope, 2000; Samet *et al*., 2000; Delfino *et al*., 2005; Laden *et al*., 2006; Franklin *et al*., 2008; Kioumourtzoglou *et al*., 2016). Long-term exposure to air pollution is responsible for the premature death of more than 1,250,000 persons annually, accounting for approximately 40% of such deaths in China (Wang *et al*., 2012). In 2013, the extreme concentration of $PM_{2.5}$ in Beijing exceeded 1000 $\mu g/m^3$, more than 40 times the health standard set by the World Health Organization (Cheng *et al*., 2011). The negative impact to residents' physical and mental health in areas covered by smog cannot be estimated. In 2012, China promulgated a new Environmental Air Quality Standard (GB3095-2012) that lists $PM_{2.5}$ as a regular key monitoring index. National monitoring of air quality conditions and the scope of pollution has continuously increased and the number of $PM_{2.5}$ concentration monitoring points increased from 612 in 2013 to 1436 in 2016. Clearly, $PM_{2.5}$ will be a key point in the prevention and control of air pollution in China in the future, and an important topic in international atmospheric environmental research.

At present, estimates of $PM_{2.5}$ spatial concentrations and characteristics are generally determined from the following data and methods (Chu *et al*., 2015). Remote sensing images retrieval for aerosol optical depth (AOD) can estimate $PM_{2.5}$ concentration, while analysis techniques include real-time data space interpolation of monitoring points, weighted regression models and mixed models. Based on these data sources and models, researchers have investigated the origin, genetic mechanism, spatial heterogeneity, transboundary transmission, health effects and coping mechanisms of $PM_{2.5}$. For example, scholars have constructed a spatio-temporal distribution and derived relationships between PM_{10} and $PM_{2.5}$ using a geographically temporally weighted regression model and cluster analysis (Yang *et al*., 2016); represented the spatial distribution of $PM_{2.5}$ using satellite retrieval for remote measurement of aerosol optical depth (AOD) (Liu *et al*., 2005; Xue *et al*., 2015); established a list of $PM_{2.5}$ discharge sources (Cao *et al*., 2011; Zhang and Cao, 2015) using an inventory-chemical mass balance model (Zhang *et al*., 2015), chemical mass balance method (Gramsch *et al*., 2006), and atmospheric diffusion model method (Austin *et al*., 2013); and revealed the spatial heterogeneity and cross-region transmission of $PM_{2.5}$ concentration using a linear regression model and Comprehensive Air Quality Model Extensions (CAM_x) air quality model for aerosol optical thickness (AOT) data (Wang *et al*., 2003; Xue *et al*., 2014). Additional studies have found that $PM_{2.5}$ concentrations show distinctive seasonal changes, but also clear geospatial heterogeneity and spatial dependence (Chow *et al*., 2006; Gelencsér *et al*., 2007; Liu *et al*., 2009; Kloog *et al*., 2012; Beckerman *et al*., 2013; Lin *et al*., 2013). Furthermore, an economic growth mode with high energy consumption and a non-ecological urbanization mode are the main factors creating high $PM_{2.5}$ in China and similar developing countries. Scholars have found that landform, meteorology, dust, transportation, biomass and coal burning were key factors affecting the spatial distribution of $PM_{2.5}$ pollution. The large-scale spatio-temporal distribution of $PM_{2.5}$ is mainly affected by global climatic change, landform and topography, population density, land utilization, economy, and traffic intensity (Charron and Harrison, 2005; Henderson *et al*., 2007; Merbitz *et al*., 2012; Gao *et al*., 2015), whereas small-scale spatio-temporal changes in $PM_{2.5}$ are controlled by the distances from monitoring points to pollution sources (e.g., urban centers, bus stations, airports, factories) (Hoek *et al*., 2002).

In summary, $PM_{2.5}$ studies have mainly focused on source analysis, pollution characteristics, and health evaluation, while largely neglecting the spatio-temporal evolution of $PM_{2.5}$ and its driving forces. Furthermore, existing studies have focused on seasonal and spatial changes in $PM_{2.5}$ concentration from case studies of international metropolises or pollution-sensitive cities, such as Los Angeles, London, and Beijing; and covered relatively short time spans (Bell *et al*., 2007). A comprehensive analysis of the spatio-temporal distribution characteristics, influencing factors, and driving forces of $PM_{2.5}$ concentration based on large scales and long time frames has not been undertaken for several reasons. (1) It is difficult to obtain large-scale and long-term $PM_{2.5}$ pollution data, and continuous monitoring data may not be available. For China, the National Atmospheric Environment Monitoring System has only included $PM_{2.5}$ concentration in the monitoring index system since 2012, and no public national $PM_{2.5}$ monitoring data is available prior to 2012. (2) In European and American countries with complete $PM_{2.5}$ monitoring systems, $PM_{2.5}$ pollution does not occur nationwide, but only appears in polluted island cities, such as Los Angeles, London and adjacent areas; large-scale, continuous pollution areas have not formed. From 2000 to 2015, China was in a period of rapid urbanization and industrialization. Based on average $PM_{2.5}$ concentration data from 1999 to 2016 provided by the United States National Aeronautics and Space Administration (NASA), it is possible to analyze the spatial-temporal distribution and influencing factors of $PM_{2.5}$ concentration in continuous polluted areas of China. These data should provide an accurate, macroscopic, and long time series, reflecting changes in $PM_{2.5}$ pollution in China during this period. To a certain extent, this dataset also addressed the problem of missing macroscopic $PM_{2.5}$ concentration monitoring data during the Chinese development from 2000 to 2012. Our findings can help forming policies to adjust energy structure, guide industrial layouts, and avoid risk of pollution in the next 10–20 years. Furthermore, such a dataset can be used to resolve $PM_{2.5}$ cross-regional pollution problems, which take the administrative unit as the main body although there are isolated air pollution prevention model, and provide spatial decision references for national cross-regional pollution linkage governance.

2 Data and methods

2.1 Data sources

The research data were obtained from three sources. (1) $PM_{2.5}$ concentrations from remote sensing retrieval. This research adopts the raster data of global atmospheric $PM_{2.5}$ concentration from 1998 to 2016 published by NASA as basic research data (website) with a resolution of 0.1° (http://earthdata.nasa.gov). Because the aerosol optical depth (AOD) product from satellite remote sensing retrieval has advantages of low cost, wide spatial coverage and high simulation accuracy, and is an important index of ground $PM_{2.5}$ concentration, it has been widely applied to remote monitoring of near-surface $PM_{2.5}$. The high correlation between AOD determined by the MODIS/Terra AOD product and $PM_{2.5}$ concentration has been verified by a variety of studies. The original data are three-year average values. To calculate data reliability and stability, this study adopted intermediate year substitution; for example, the average $PM_{2.5}$ concentration from 2014 to 2016 is taken as the average $PM_{2.5}$ concentration of 2015. (2) Basic geographic information data and spatial administrative boundaries were derived from 1:4 million Chinese basic geographic information data provided by the National Basic Geographic Information Center. Taking the full territory of the People's Republic of China (including Mainland of China, Hong Kong, Macao and Taiwan) as the research area, the grid data was then extracted using the research area vector boundary as a mask. The average $PM_{2.5}$ concentration was calculated for each year in each county-level administrative unit, which established the spatio-temporal database for $PM_{2.5}$ concentration in China based on the county-level administrative region boundaries. (3) Socioeconomic data, car ownership, population density, and straw burning were obtained from the *China City Statistical Yearbook*, *China Urban Construction Statistical Yearbook*, *China Region Statistical Yearbook*, and *China Rural Statistical Yearbook* in each corresponding year from 2000 to 2016; some missing data were supplemented from data of corresponding provinces (autonomous regions) and municipalities.

2.2 Methodology

2.2.1 Gravity model

Tobler's first law of geography considers that geographical things or properties are mutually related in terms of spatial distributions, i.e., clustering, random, and regularity. Specifically, neighbouring objects and properties are more related than distant objects, termed spatial autocorrelation (Wang *et al*., 2015). To thoroughly analyze the spatio-temporal distribution patterns and characteristics of $PM_{2.5}$, this study first introduces the concept of center of gravity and a calculation method to reveal the $PM_{2.5}$ spatial migration process. This gravity model is used as a representation of changing spatial cluster characteristics of $PM_{2.5}$, and

Moran's I index is used as a representation of the spatial agglomeration characteristics of $PM_{2.5}$. The coordinates X and Y of the center of gravity of $PM_{2.5}$ pollution are calculated as:

$$\overline{X}=\frac{\sum_{i=1}^{n}W_i\times S_i\times X_i}{\sum_{i=1}^{n}W_i\times S_i} \quad \text{and} \quad \overline{Y}=\frac{\sum_{i=1}^{n}W_i\times S_i\times Y_i}{\sum_{i=1}^{n}W_i\times S_i} \tag{1}$$

where $\overline{X}$ is the longitude of $PM_{2.5}$ pollution gravity. $\overline{Y}$ is the latitude of $PM_{2.5}$ pollution gravity. n indicates the raster quantity and i indicates the raster number. X_i and Y_i indicate the longitude and latitude of the geometric center of raster i, respectively. S_i indicates the area of raster i, and W_i indicates the annual average $PM_{2.5}$ concentration of raster i.

2.2.2 Spatial autocorrelation

This study applies global Moran's index (Global Moran's I) to test the global spatial autocorrelation of $PM_{2.5}$ concentration. If the Global Moran's I index is greater than 0, the research object has a positive spatial autocorrelation, and a larger value indicates a stronger spatial agglomeration of the observed $PM_{2.5}$ value. When the Global Moran's I index is less than 0, the $PM_{2.5}$ concentration presents a negative spatial autocorrelation, and a smaller value indicates a stronger spatial dispersion of the observed value. The Global Moran's I index is calculated as:

$$I=\frac{\sum_{i=1}^{n}\sum_{j=1}^{n}W_{ij}\left(x_i-\overline{x}\right)\left(x_j-\overline{x}\right)}{S^2\sum_{i=1}^{n}\sum_{j=1}^{n}W_{ij}} \tag{2}$$

$$S=\frac{1}{n}\sum_{i=1}^{n}\left(x_i-\overline{x}\right)^2 \tag{3}$$

where n indicates the quantity of spatial units (county-level administrative units are adopted in this study). X_i and X_j are the annual average $PM_{2.5}$ concentration of units i and j, respectively, and $\overline{X}$ indicates the average value of all units. W_{ij} indicates the spatial weight matrix of units i and j; if there is a common edge between spatial units i and j, then $W_{ij}=1$, otherwise, $W_{ij}=0$. To test the significance of the Global Moran's I index, the standardized normalization value of the Global Moran's I index, $Z(I)$, is defined as follows:

$$Z\left(I\right)=\frac{\left[I-E(I)\right]}{\sqrt{Var(I)}} \tag{4}$$

where $E(I)$ indicates the mathematical expectation of the Global Moran's I index, and $Var(I)$ indicates the variance in the Global Moran's I index.

The Local Moran's I index is applied to extract the local spatial autocorrelation of atmospheric $PM_{2.5}$ pollution and identify spatial agglomeration and heterogeneity. For the spatial unit i, the Local Moran's I index is defined as:

$$I_i=\frac{\sum_{i=1}^{n}\sum_{j=1}^{n}W_{ij}\left(x_i-\overline{x}\right)\left(x_j-\overline{x}\right)}{S^2} \tag{5}$$

where $Z(I)$ still indicates the significance level of the Local Global Moran's I index, calculated from equation (4). $Z(I)$ values are compared at different levels by dividing spatial units into four types of spatial autocorrelation based on threshold (p=0.05 in this study). When I is significantly positive and $Z(I)>0$, it is termed a "high-high" type and indicates that the $PM_{2.5}$ concentration of this unit and adjacent units are relatively high, i.e., a hot spot. When I is significantly positive and $Z(I)<0$, it is termed a "low-low" type and indicates that the $PM_{2.5}$ concentration of this unit and adjacent units are relatively low, i.e., a cold spot. When I is significantly negative and $Z(I)>0$, it is termed a "high-low" type and indicated that high concentration of $PM_{2.5}$ units are surrounded by low adjacent units. When I is significantly negative and $Z(I)<0$, it is termed a "low-high" type and indicates that low concentration of $PM_{2.5}$ units are surrounded by high adjacent units. A significantly positive I indicates that there is significantly local spatial positive autocorrelation and spatial clustering. A significantly negative I indicates that there is significantly local negative spatial autocorrelation and spatial dispersion.

2.2.3 Geographic detector

Geographic detection is a set of statistical methods to detect the spatial heterogeneity and reveal driving forces; it is an important method for detecting the causes and mechanism of spatial patterns of geographical factors and has been applied to the studies of disease risk detection, socio-economy, and eco-environment (Liu *et al*., 2012; Wang *et al*., 2017; Lindner, 2018). The factor detector in the model is used to identify a specific geographical factor and quantify the spatial distribution difference by comparing the total variance of this index in different types of areas and in the whole area. The model is defined as:

$$P_{D,H}=1-\frac{1}{n\sigma_H^2}\sum_{i=1}^{n}n_{D,i}\sigma\frac{2}{H_{D,j}} \tag{6}$$

where $P_{D,H}$ indicates the explanatory power of the influencing factor of $PM_{2.5}$; D indicates the factors influencing annual average $PM_{2.5}$ concentration; n and σ^2 indicate the overall sample quantity and variance of the research area, respectively; m indicates the number of categories for the factors; and $n_{D,i}$ indicates the number of D indices on category-i samples. $P_{D,H}$ ranges from 0 to 1, and a larger value indicates a stronger explanatory power of this factor for a change in $PM_{2.5}$ concentration. When the value is 0, the classification factor is completely unrelated to the change in $PM_{2.5}$ concentration. When the value is 1, the classification factor can completely explain the change in the spatial distribution of $PM_{2.5}$ concentration.

3 The spatio-temporal evolution characteristics of $PM_{2.5}$ pollution

3.1 Time series characteristics of $PM_{2.5}$

Based on a comprehensive time analysis and Spearman rank correlation coefficient analysis, the annual average $PM_{2.5}$ concentration in China rose steadily from 2000 to 2015, a trend that was not identified in the monitoring data (Figure 1). The annual average $PM_{2.5}$ concentration increased from 21.84 μg/m^3 in 2000 to 35.08 μg/m^3 in 2006, with an average annual increase of 1.66 μg/m^3; this was a significant rising trend in this stage (p=0.05). The $PM_{2.5}$ concentration has generally fluctuated around 32.57 μg/m^3 since 2006, and the significant upward trend leading to 2006 has stabilized to a certain degree. This indicates that 2006 was a turning point in $PM_{2.5}$ annual average concentration change in China. This result is consistent with results published by China's Ministry of Environmental Protection in 2007. The national ecological civilization construction, ecological supplement points, pollution survey and the achievement of environmental protection policies, the adjustment of industrial structure and improvements in energy efficiency have restrained the $PM_{2.5}$ emissions to a certain extent. However, the annual average $PM_{2.5}$ concentration in China still remained high. The raster of annual $PM_{2.5}$ concentration in 2015 increased by 39.76% compared to 2000. Furthermore, 13.20% of rasters had annual average concentrations that approximately doubled, indicating that $PM_{2.5}$ pollution continues to expand across the national land space.

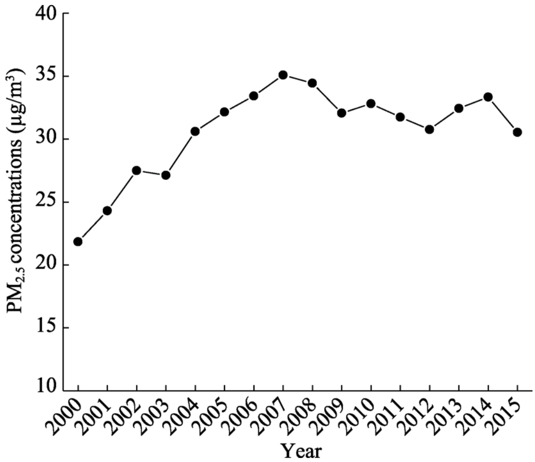

Figure 1 Overall $PM_{2.5}$ concentration trend in China from 2000 to 2015

Based on the annual average concentration limit of $PM_{2.5}$ in the Ambient Air Quality Standard (GB3095-2012) of China (Samet *et al.*, 2000), the annual average $PM_{2.5}$ concentration was divided into seven intervals and the area proportion of each interval was analyzed for the study period (Figure 2). Four important results were obtained. (1) The proportion of annual average $PM_{2.5}$ concentration lower than 15 μg/m^3 (the first-order concentration limit) decreased continuously from 28.95% in 2000 to 91.21% in 2015. (2) The proportion of annual average $PM_{2.5}$ concentration higher than 35 μg/m^3 (the second-order concentration limit) increased from 17.78% in 2000 to 32.89% in 2015. (3) The proportion of high-pollution areas with annual average $PM_{2.5}$ concentration higher than 70 μg/m^3 increased greatly from 0.04% in 2000 to 4.06% in 2015, and the increase was more than 100 times larger. (4) The high-pollution areas with annual average $PM_{2.5}$ concentration higher than 100 μg/m^3

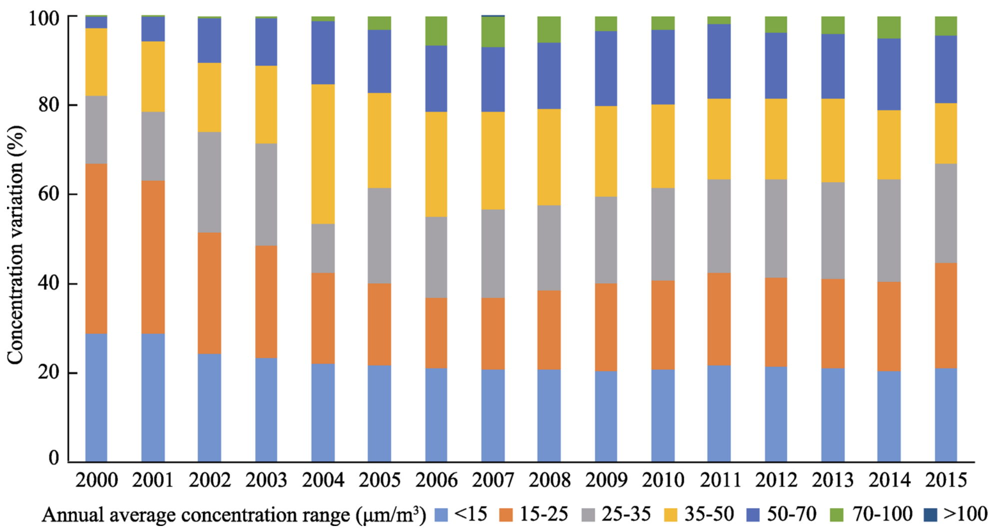

Figure 2 Variations in $PM_{2.5}$ concentration by range in China from 2000 to 2015

emerged in large numbers from 2006 to 2007 and from 2010 to 2015, and the proportion in other years was lower than 0.50%. These results indicate that low-pollution areas with annual average $PM_{2.5}$ concentration lower than 15 μg/m^3 decreased continuously, while high-pollution areas with annual average $PM_{2.5}$ concentration higher than 70 μg/m^3 increased. High-pollution areas and extremely high-pollution areas showed a rapid expansion in the national space.

3.2 Characteristics of spatio-temporal patterns in China

3.2.1 Spatial variations

Identifying the $PM_{2.5}$ spatial evolution characteristics and distribution and exploring changes in $PM_{2.5}$ concentrations in the national space have importance implications for controlling cross-regional linkage pollution in China. The primary spatial characteristics of $PM_{2.5}$ in China for 2000–2015 were obtained by analyzing the $PM_{2.5}$ grid data. In areas with annual average $PM_{2.5}$ concentration higher than 100 μg/m^3, the pollution was extremely serious (Figure 3), which only appeared in counties, such as Xinxiang and Yanjin in Henan Province, in 2000. However, serious pollution began to extend into and cover parts of northern Henan and southern Hebei provinces in 2008 and was distributed sporadically in the Fenhe-Weihe Basin and Sichuan Basin. High-pollution areas with annual average $PM_{2.5}$ concentration higher than 70 μg/m^3 were distributed continuously in the North China Plain, Fenhe-Weihe Basin and Sichuan Basin. The high-pollution area in the North China Plain was the largest and spread across the midstream and downstream plains of the Yangtze River. In addition to the densely populated and economically developed areas, high-pollution areas were distributed sporadically in the Tarim Basin. With the exceptions of Heilongjiang, Yunnan, Fujian, Taiwan, and Hainan, the annual average $PM_{2.5}$ concentration in areas east of the Heihe-Tengchong Line generally exceeded 35 μg/m^3; the annual average $PM_{2.5}$ concentration in the most densely populated areas in China did not meet the secondary standard of the

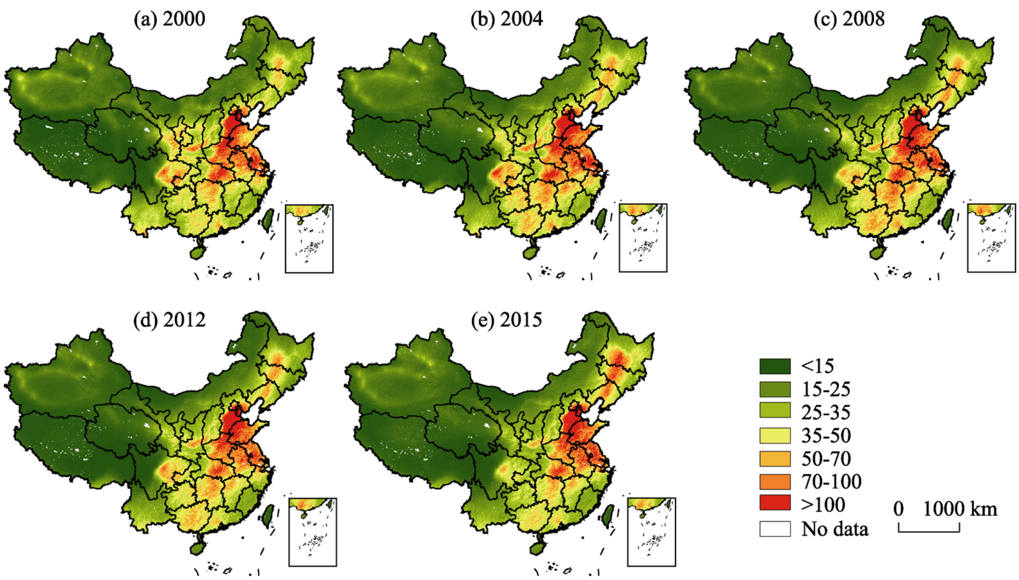

Figure 3 $PM_{2.5}$ spatial characteristics in China in specific years from 2000 to 2015

Ambient Air Quality Standard. Finally, in the areas west of the Heihe-Tengchong Line, with the exception of the Tarim Basin, which is subject to the influences of airborne dust from the Taklimakan Desert in spring, the annual average $PM_{2.5}$ concentration is generally lower than 35 μg/m^3. Areas with relatively serious $PM_{2.5}$ pollution are mainly concentrated in North China and the Yangtze River Basin area. The $PM_{2.5}$ pollution had close relationships with geographically low-lying plains and population density and economic activity.

3.2.2 Spatio-temporal evolution

To describe the spatial characteristics of $PM_{2.5}$ concentration change and pollution, the county-level administrative division was used as the basic unit and grids were used to calculate detailed statistics for 2853 counties for four stages, 2000–2004, 2004–2008, 2008–2012 and 2012–2015. Changes in concentrations, i.e., rise (R) and decline (D), for the four stages were used to divide the variation in $PM_{2.5}$ concentrations into 16 types of time sequences for evaluation (Table 1 and Figure 4). During the research period, the county-level units with continuous increases in $PM_{2.5}$ accounted for 7.15% of the total units and were mainly distributed in Tibet and Northeast China, where $PM_{2.5}$ pollution was not as serious. These regions had relatively good eco-environment, but the air quality deteriorated continuously, which is worthy of national attention. From 2000 to 2008, the county-level research units with continuous increases in degree of $PM_{2.5}$ pollution accounted for 82.55% of all units, indicating $PM_{2.5}$ pollution aggravation in most regions of China. This has been characterized as one of the fastest industrialization and urbanization periods in China. The distributions of time sequence trends showed clear spatial agglomeration; for example, D-R-D-R was concentrated in the Shaanxi, Gansu and Ningxia regions, whereas D-D-R-R was generally distributed in the Southern Xinjiang region. Only four counties showed continuously falling $PM_{2.5}$, which were distributed in Jiuquan, Gansu Province.

Table 1 Distribution chart of 16 types of time sequences of $PM_{2.5}$ concentration evolution in China

No.	Change type	Quantity	%	No.	Change type	Quantity	%
1	D—D—D—D	4	0.17	9	R—D—D—D	38	1.59
2	D—D—D—R	5	0.21	10	R—D—D—R	71	2.97
3	D—D—R—D	11	0.46	11	R—D—R—D	120	5.02
4	D—D—R—R	1	0.04	12	R—D—R—R	68	2.85
5	D—R—D—D	45	1.88	13	R—R—D—D	811	33.93
6	D—R—D—R	13	0.54	14	R—R—D—R	801	33.51
7	D—R—R—D	36	1.51	15	R—R—R—D	190	7.95
8	D—R—R—R	5	0.21	16	R—R—R—R	171	7.15

Note: R indicates rise, and D indicates decline.

3.2.3 Movement of center of gravity

The center of gravity movement for $PM_{2.5}$ in China from 2000 to 2015 calculated from equation (5) showed significant trends. During the study period, the center of gravity was located at the juncture of Shaanxi and Henan provinces (Figure 5). However, the center of gravity moved southward at an average of 24.97 km annually from 2000 to 2004, showing a clear increase in $PM_{2.5}$. The movement slowed after 2005 and the average annual movement distance decreased to 15.04 km. In 2001, the center of gravity for high concentration $PM_{2.5}$

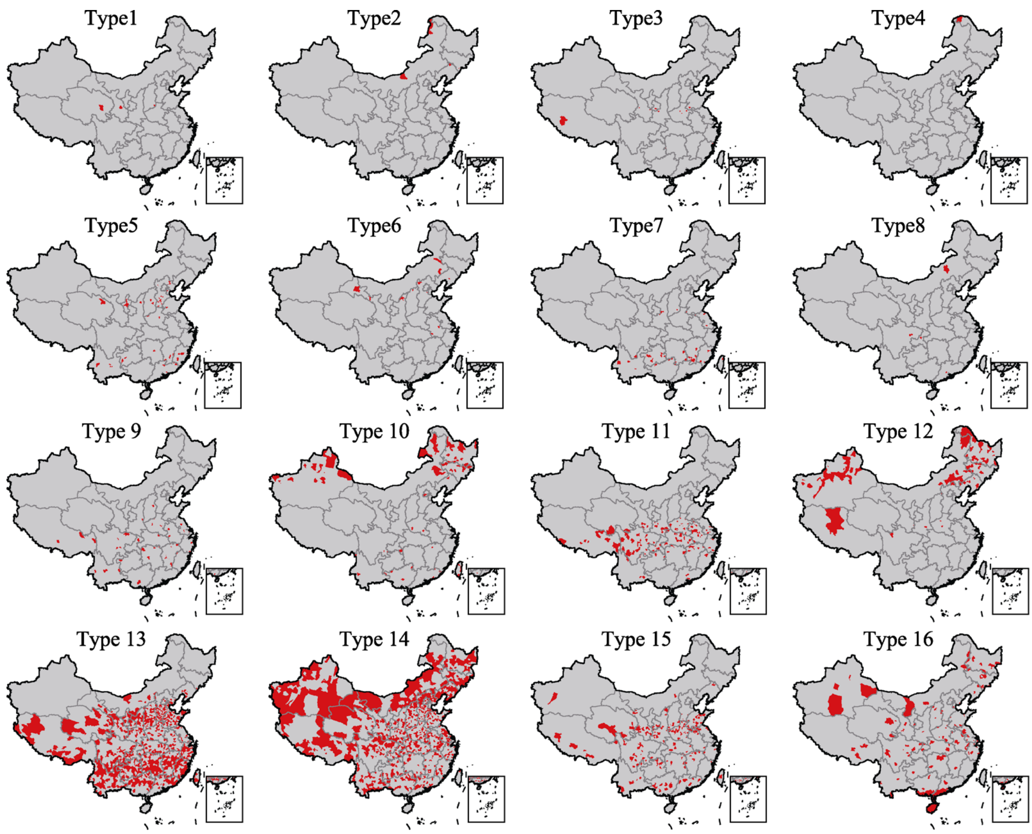

Figure 4 The evolution of $PM_{2.5}$ concentrations for the 16 time sequences in China (see Table 1 for time sequence definitions)

moved rapidly from southwest to northeast and was located in Shaanxi Province. It subsequently moved quickly to Henan Province with an average annual distance of 156.09 km from 2001 to 2003. After 2004, it returned to Shaanxi Province, but the movement distance rapidly dropped to 40.71 km after 2004, showing a relatively steady state. In contrast, the center of gravity for low concentration $PM_{2.5}$ moved westward rapidly. The center of gravity was located in Inner Mongolia for a long time and showed a common direction with the high concentration center of gravity. The average annual movement distance before 2004 was 86.37 km, which decreased to 37.84 km from 2005 to 2015. Generally, the center of gravity for the overall and high concentration $PM_{2.5}$ showed movement to the northeast, while the center of gravity for low concentration $PM_{2.5}$ moved westward. All three centers of gravity moved rapidly

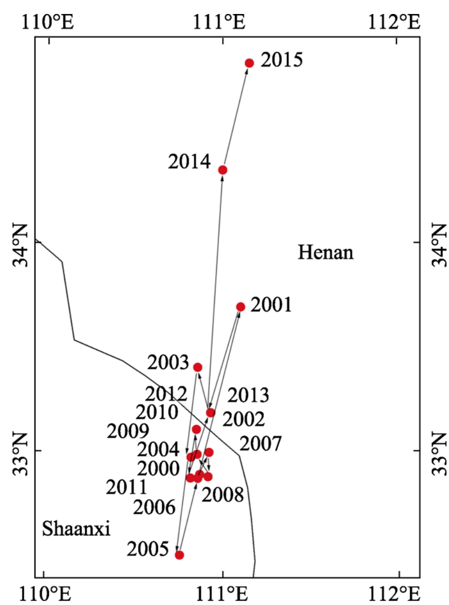

Figure 5 Changes in $PM_{2.5}$ concentration center of gravity in China from 2000 to 2015

before 2004 and tended to stabilize after 2005. This change is closely related to the enhancement of national ecological civilization construction, industrial transfer (eastern to central and western regions), and higher thresholds for environmental protection in eastern China. These results are in agreement with those presented in section 3.1, indicating that the $PM_{2.5}$ pollution in the eastern region was higher than that in the western region and higher in the northern region than in the southern.

3.3 Spatial autocorrelation analysis

3.3.1 Global spatial autocorrelation

The Global Moran's *I* index of the annual average $PM_{2.5}$ concentration in each county-level unit from 2000 to 2015 was positive and passed the significance test (p=0.05). Therefore, the annual average $PM_{2.5}$ concentration presented a significant positive spatial autocorrelation and showed an agglomerated spatial pattern. From the time sequence, the Global Moran's *I* index reached a maximum in 2006 and then generally decreased year after year. This turning point is consistent with the turning point in annual average concentration, indicating that the spatial agglomeration of the annual average $PM_{2.5}$ concentration first increased and then decreased, and the degree of spatial agglomeration reached its peak in 2006.

3.3.2 Local spatial autocorrelation

Based on local spatial autocorrelation analysis results (Figure 6), the county-level units presenting significant local spatial autocorrelation were divided into four types: high-high, low-low, high-low, and low-high. The high-high areas with high annual average $PM_{2.5}$ concentration, i.e., the hot spots for $PM_{2.5}$ pollution, were continuously distributed in the North China Plain, Fenhe-Weihe Basin, Sichuan Basin, and Jianghan Plain regions. The number of county-level administrative units contained in the hot spots was generally unchanged from 2000 to 2004, but increased greatly from 2006 to 2009, and then decreased in 2008. The low-low areas with low annual average $PM_{2.5}$ concentration, i.e., the cold spots for $PM_{2.5}$

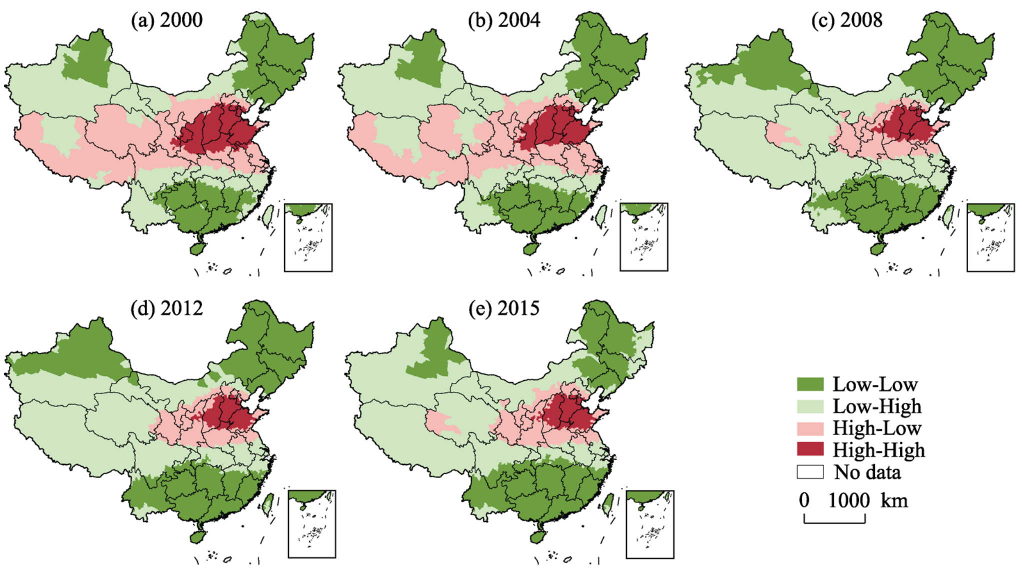

Figure 6 Local spatial autocorrelation analysis results for $PM_{2.5}$ in China from 2000 to 2015

pollution, were distributed continuously in the northern part of Northeast China, Taiwan, Yunnan, Qinghai-Tibet Plateau, Xinjiang, the northern part of Inner Mongolia, and other border areas. The number of county-level administrative units contained in the cold spots was similar to the number of hot spots in terms of change over time; generally, unchanged before the distinctive increase in 2012 and then dropped to a minimum in 2015. The other county-level administrative units did not present significant local spatial autocorrelation. During the research period, no county-level administrative units of high-low or low-high local spatial autocorrelation types were identified, indicating that the annual average $PM_{2.5}$ concentration had strong local positive spatial autocorrelation characteristics.

4 Driving forces of $PM_{2.5}$ pollution

Spatial variations in $PM_{2.5}$ concentration in China were significant. However, the origins are complicated and the factors affecting changes in pollution concentrations are diverse and include natural factors, such as atmospheric circulation, volcano ash, forest fires, flying dust in bare desert areas, wind direction and frequency, and rainfall. Anthropogenic factors include industrial flue dust discharge, coal combustion, straw burning, exhaust from motor vehicles, flying dust from construction site. To analyze the factors contributing to changes in $PM_{2.5}$ concentrations more comprehensively, we selected panel data for 287 prefecture-level cities in 2000, 2006, and 2011, including a total of 27,839 samples. We adopted the geographical detector method to detect characteristics of spatial differentiation and identify the driving forces. We chose the following 11 index factors as contributing to high $PM_{2.5}$ concentrations in the data sources described in the methods section: natural geographical regionalization (X_1), per capita GDP (X_2), population density (X_3), proportion of secondary industry (X_4), proportion of built-up areas (X_5), urban greening ratio (X_6), urban residents' car ownership (X_7), sown area (X_8), industrial flue dust discharge (X_9), average energy consumption intensity (X_{10}), average iron and steel output of lands (X_{11}). We then calculated their degrees of influence on the spatial distributions of $PM_{2.5}$ in 287 prefecture-level Chinese cities (Table 2).

Table 2 Geographical detection results for $PM_{2.5}$ in China for 2000, 2006, and 2011

Detection indices	2000		2006		2011	
	P	Q	P	Q	P	Q
Natural geographical regionalization (X_1)	0.7047	0.0000	0.7447	0.0000	0.7196	0.0000
Per capita GDP (X_2)	0.0077	0.9191	0.0062	0.9079	0.0068	0.8659
Population density (X_3)	0.4320	0.0000	0.4372	0.0000	0.4120	0.0000
Proportion of the secondary industry (X_4)	0.0984	0.0000	0.0665	0.0031	0.0917	0.0000
Proportion of built-up areas (X_5)	0.0853	0.0030	0.0753	0.1033	0.1025	0.0282
Urban greening ratio (X_6)	0.0280	0.1503	0.0625	0.0319	0.0359	0.1083
Urban residents' car ownership (X_7)	0.0259	0.8637	0.0913	0.0226	0.1074	0.0080
Sown area (X_8)	0.1396	0.0557	0.1487	0.0000	0.1046	0.0000
Industrial flue dust discharge (X_9)	0.0709	0.1537	0.0936	0.0000	0.0531	0.2766
Energy consumption intensity of lands (X_{10})	0.3109	0.0000	0.4124	0.0000	0.4143	0.0000
Average iron and steel output of lands (X_{11})	0.2869	0.0000	0.3373	0.0000	0.3217	0.0000

4.1 Natural factors affecting $PM_{2.5}$ spatio-temporal evolution

The geographical detection results indicate that changes in $PM_{2.5}$ concentrations are closely related to regional natural factors. Natural geographical regionalization (X_1) has the most significant influence on $PM_{2.5}$. In the three selected years (2000, 2006, and 2011), its detection and explanatory power P for $PM_{2.5}$ were 0.7047, 0.7477, and 0.7196, respectively, indicating large-scale regional differentiation and significant influence from landform, climate, hydrology, soil and vegetation on the formation mechanism of $PM_{2.5}$. Among the four areas suffering serious $PM_{2.5}$ pollution, also recognized in section 3.2.1 in this paper, the change of $PM_{2.5}$ in Taklimakan Desert was closely related to the regional atmospheric circulation and local sand-dust weather. Observations from 88 monitoring stations in Xinjiang from 2000 to 2011 show that the Taklimakan Desert and its southern edge were sand-dust weather frequently observed area with sand-dust days 2.7 times more in Southern Xinjiang than in the Northern (Jiang *et al*., 2013); therefore, $PM_{2.5}$ concentrations showed spatial coupling characteristics that were higher in Southern Xinjiang than in the Northern. The overall increase in vegetation coverage and change in rainfall in Xinjiang also affected the change in $PM_{2.5}$ in the Taklimakan Desert to a certain degree. Moreover, influenced by ocean currents, the southeast monsoon, warm and humid climate, high precipitation, dense population, and industrial agglomeration, the Pearl River Delta and island regions (e.g., coastal Fujian, Taiwan and Hainan) showed relatively low annual average $PM_{2.5}$ concentration and were not severely polluted. Similarly, regions such as the Qinghai-Tibet Plateau, Inner Mongolia Plateau, and Yunnan-Guizhou Plateau with rugged landforms had few human activities; thus, the $PM_{2.5}$ concentrations have remained relatively low.

4.2 Socio-economic factors affecting the spatio-temporal evolution in $PM_{2.5}$

Increases in human activity has a strong impact on air pollution, including flying dust arising from urbanization, emissions due to more private cars, increases in energy consumption, coal-fired heating facilities due to sharp rises in population, and straw burning caused by agricultural production. Excluding Xinjiang, which is strongly affected by natural factors, the three regions with high $PM_{2.5}$ concentration were generally consistent with the spatial distribution of population density in China. The geographical detection results indicate that the regions suffering serious $PM_{2.5}$ pollution were mainly concentrated in densely populated regions, including the North China Plain, with Beijing-Tianjin-Hebei region as the center; Shandong Peninsula; Hunan-Hubei Plain; and Chengdu-Chongqing Basin. A quantitative analysis of each factor influencing $PM_{2.5}$ concentration is as follows.

(1) Driven by urban construction. Based on geographical detection, the detected p values for urban development and construction influence on $PM_{2.5}$ concentration in 2000, 2006, and 2011 were 0.4320, 0.4372, and 0.4120, respectively. Population density contributed the most to the changes in $PM_{2.5}$ concentration, characterized by an inverted U-shaped pattern. The detected p values for the proportion of built-up areas (X_5) in 2000, 2006, and 2011 were 0.0853, 0.0753, and 0.1025 respectively, and their contributions to the changes in regional $PM_{2.5}$ concentration increased gradually with the acceleration in urban construction. The detected p values for the urban greening ratio (X_6) in 2000, 2006, and 2011 were 0.0280, 0.0625, and 0.0359, respectively, and their contributions to changes in regional $PM_{2.5}$ concentration were also characterized by an inverted U-shaped pattern. Urban greening can mitigate dust and relieve its effect on $PM_{2.5}$ in the atmosphere to a certain degree; however, the influence was minor. Similarly, per capita GDP (X_2) had a relatively small influence.

(2) Driven by industry and energy (coal) consumption. In 2000, 2006 and 2011, the detected p values for the proportion of secondary industry (X_4) were respectively 0.0984, 0.0665, and 0.0917; those of the average energy consumption intensity of lands (X_{10}) were respectively 0.3109, 0.4124, and 0.4143, and those of the average iron and steel output of lands (X_{11}) were respectively 0.2869, 0.3373, and 0.3217. Both industry and coal consumption were significant factors in $PM_{2.5}$ pollution (significance level = 0.01), indicating that emission of particulate pollutants in cities is the dominant source of pollution to most cities and regions. From 2000 to 2011, the total energy consumption in China increased by 2.39, and the proportion of coal to total energy consumption only decreased from 69.21% in 2000 to 68.42% in 2011; that is, coal remained the primary source of energy in China. In 2015, coal still accounted for 68% of all energy consumed with no substantial decline. Total coal consumption in high polluted areas, such as Shandong, Inner Mongolia, Shanxi, Hebei, Henan, and Jiangsu exceeded 200 million tons. From 2000 to 2011, the iron and steel industry consumed a huge quantity of coal resources in China, primarily in three regions, the Yangtze River Delta, North China Plain, and Sichuan Basin; these areas are iron and steel industry concentrated areas. In these regions, ten provinces and cities, including Hebei, Tianjin, Shandong, Shaanxi, Jiangsu, Liaoning, Shanghai, and Sichuan, host the majority of iron and steel industries in China. In 2011, the crude steel output of these ten provinces and cities was 4945 million tons, accounting for 70.44% of the national output in that year. Therefore, coal consumption and spatial distribution of iron and steel industries are key factors affecting changes in $PM_{2.5}$ concentration.

(3) Driven by the exhaust emissions of motor vehicles. In 2000, 2006 and 2011, the detected p values for civil car ownership (X_7) were 0.0984, 0.0665, and 0.0917, respectively, and car ownership had insignificant effects on $PM_{2.5}$ concentration in 2000 and 2006. However, with the sharp increase in the number of cars after 2006, the effect of car ownership became significant in 2011. From 2000 to 2011, civil car ownership in China increased by 5.82 times and private car ownership increased by 11.72 times. The growth in car ownership was far higher than economic growth (4.77 times), per capita income (4.48 times), and highway mileage (2.45 times). In provinces and cities suffering serious haze pollution, e.g., Beijing, Hebei, Jiangsu, Zhejiang, and Shandong, the total numbers of civilian vehicles all exceed 4,000,000 per region.

(4) Driven by straw burning. In 2000, 2006 and 2011, the detected p values for the influence of sown area of farm crops (X_8) on $PM_{2.5}$ were 0.1396, 0.1487, and 0.1046, respectively. These were also characterized by an inverted U-shaped change pattern and the influence of straw burning on regional $PM_{2.5}$ concentration reached a maximum in 2006. The total agricultural straw in China was 6×10^8 t, and 18.59% of straw was burnt in open space in rural areas. The pollution arising from straw burning was less than 5% of total $PM_{2.5}$. However, the locations were agglomerated primarily in Eastern and Northern China regions with developed agriculture, and the time of burning was concentrated, with the peak occurring around October for 1–2 days. Therefore, $PM_{2.5}$ arising from straw burning possibly accounted for 30% or 40% of the total $PM_{2.5}$ in the air on specific days and had significant influence on regional air pollution (Lu *et al*., 2011).

5 Conclusions and implications

5.1 Conclusions

(1) Time sequence and Spearman rank correlation coefficient analysis shows that the annual average $PM_{2.5}$ concentration in China was high throughout the study period. From 2000 to 2015, the $PM_{2.5}$ concentration in China first increased rapidly and then became stable; 2006 was identified as a turning point for the overall change in $PM_{2.5}$ concentration in China. However, the annual average $PM_{2.5}$ concentration in China was high and presented a trend of obvious diffusion in national land space. In 2011, the proportion of annual $PM_{2.5}$ concentration raster to total raster increased by 75.12% compared to 2000, and the raster with growth rates showing a doubling of annual average concentration accounted for 13.20%.

(2) Spatial analysis shows that northern and eastern China had higher concentrations than southern and western China; the Heihe-Tengchong Line is the significant dividing line. $PM_{2.5}$ pollution concentration areas and extremely polluted areas showed clear expansion. The areas with average concentrations less than 15 μg/m^3 decreased while areas with average concentrations more than 70 μg/m^3 increased. Areas with high $PM_{2.5}$ pollution concentrations were distributed in the North China Plain, and were related to low-altitudes. County-level administrative analyses indicate that $PM_{2.5}$ pollution rose in 76.23% county-level administrative units from 2000 to 2006. The increase of $PM_{2.5}$ pollution during this period was the general trend in most regions.

(3) The center of gravity for $PM_{2.5}$ pollution in China is located in eastern Shaanxi; from 2000 to 2004, the center of gravity moved eastward at 24.97 km annually. After 2004, the center of gravity for high-pollution-concentration areas moved eastward, while the low-pollution center of gravity moved westward. The movement in opposite directions indicates that $PM_{2.5}$ pollution in the eastern regions clearly increased in this period and eastern $PM_{2.5}$ pollution increased more than western. Spatial autocorrelation analysis shows that the annual average $PM_{2.5}$ concentration was strongly characterized by local spatial positive autocorrelation. The "high-high" $PM_{2.5}$ agglomeration areas were distributed continuously in the North China Plain, Fenhe-Weihe Basin, Sichuan Basin and Jianghan Plain regions; "low-low" $PM_{2.5}$ agglomeration areas were distributed in northern Inner Mongolia and Heilongjiang; the southeast coastal and island regions, e.g., Taiwan, Hainan, and Fujian; and the border areas, e.g., the Qinghai-Tibet Plateau and northern Xinjiang.

(4) An evaluation of the driving forces of $PM_{2.5}$ pollution in China indicates that natural factors and human economic activities have both affected the spatial characteristics and concentrations of $PM_{2.5}$. The influence of natural geographical division on $PM_{2.5}$ is most significant, and the detected p values for the three stages of the study period were higher than 0.7240. In addition, atmospheric condition, population growth (population density), industrial emission, straw burning, energy consumption growth, increases in motor vehicle ownership increased, and increases in car exhaust over the short term are the main driving forces for changes in $PM_{2.5}$ concentration in China.

5.2 Implications

Quantitatively identifying the spatial variation and regularity of $PM_{2.5}$ concentrations and evaluating the driving forces and mechanism of changes in $PM_{2.5}$ concentration are keys to developing the economy while protecting the environment. These efforts can relieve residents' psychological fear that "haze is to be even more dreaded than tigers," while also providing a scientific basis for regional atmospheric linkage prevention and control, a spatial configuration for heavy-polluting industries, designing urban landscapes (wind pipe, greenway), and adjusting industrial and energy structures. Due to data limitations, studying the large-scale evolution in $PM_{2.5}$ concentrations began late in China. Existing studies have been primarily based on data from environmental monitoring locations and involved analyses of quarterly and daily changes using one-year segment data. This study used average $PM_{2.5}$ concentration data from 1999 to 2016 provided by NASA to address the problems created by limitations in large-scale $PM_{2.5}$ data from 2000 to 2015 in China, i.e., the limited monitoring stations in the central and western regions and limited research on regional information distortion. The spatial distribution patterns in $PM_{2.5}$ concentrations presented here are consistent with previous studies (Zhang, 2015; Wang, 2015) and agree with the spatial characteristics of monitoring points in the sparse areas, although for a longer period. However, the factors affecting $PM_{2.5}$ concentration in China are complicated. Natural factors include atmospheric circulation, extreme weather, landform, and regional transfer. Anthropogenic factors include industrial pollution, coal burning, motor vehicle emission, dust, biomass burning, car exhaust and waste burning, which are the most important driving forces. Due to the large gap between industrial structure, energy structure and consumption structure in various regions or cities, China is in a key period of economic transformation described as "adjusting structure, stabilizing growth and development in green." Predicting the complexity of atmospheric pollutants to provide long-term administration includes key scientific issues, such as "reasons and control of atmospheric haze" and "the relationship between haze and health" that the country must address and are also the focus of future research and exploration.

References

Austin E, Coull B A, Zanobetti A *et al*., 2013. A framework to spatially cluster air pollution monitoring sites in US based on the $PM_{2.5}$ composition. *Environment International*, 59(3): 244–254.

Beckerman B S, Jerrett M, Serre M *et al*., 2013. A hybrid approach to estimating national scale spatiotemporal variability of $PM_{2.5}$ in the contiguous United States. *Environmental Science & Technology*, 47(13): 7233–7241.

Bell M L, Dominici F, Ebisu K *et al*., 2007. Spatial and temporal variation in $PM_{2.5}$ chemical composition in the United States for health effects studies. *Environmental Health Perspectives*, 115(7): 989–995.

Cao G L, Zhang X Y, Gong S L *et al*., 2011. Emission inventories of primary particles and pollutant gases for China. *Atmospheric Environment*, 45(37): 6802–6811. (in Chinese)

Charron A, Harrison R M, 2005. Fine ($PM_{2.5}$) and coarse ($PM_{2.5–10}$) particulate matter on a heavily trafficked London highway: Sources and processes. *Environmental Science & Technology*, 39(20): 7768–7776.

Cheng S, Yang L X, Zhou X *et al*., 2011. Evaluating $PM_{2.5}$ ionic components and source apportionment in Jinan, China from 2004 to 2008 using trajectory statistical methods. *Journal of Environmental Monitoring*, 13(6): 1662–1671.

Chow J C, Chen L W, Watson J G *et al*., 2006. $PM_{2.5}$ chemical composition and spatiotemporal variability during the California regional PM_{10}/$PM_{2.5}$ air quality study (CRPAQS). *Journal of Geophysical Research Atmospheres*, 111(D10): 1–17.

Chu H J, Huang B, Lin C Y, 2015. Modeling the spatio-temporal heterogeneity in the PM_{10}-$PM_{2.5}$ relationship. *Atmospheric Environment*, 102(2): 176–182.

Delfino R J, Sioutas C, Malik S, 2005. Potential role of ultrafine particles in associations between airborne particle mass and cardiovascular health. *Environmental Health Perspectives*, 113(8): 934–946.

Dockery D W, Pope CA, Xu X *et al*., 1994. An association between air pollution and mortality in six US cities. *New England Journal of Medicine*, 329(24): 1753–1759.

Franklin M, Koutrakis P, Schwartz P, 2008. The role of particle composition on the association between $PM_{2.5}$ and mortality. *Epidemiology*, 19(5): 680–689.

Gao M, Cao J, Seto E. A, 2015. A distributed network of low-cost continuous reading sensors to measure spatio-temporal variations of $PM_{2.5}$ in Xi'an, China. *Environmental Pollution*, 199(4): 56–65.

Gelencsér A, May B, Simpson D *et al*., 2007. Source apportionment of $PM_{2.5}$ organic aerosol over Europe: Primary/secondary, natural/anthropogenic, and fossil/biogenic origin. *Journal of Geophysical Research Atmospheres*, 112(D23): 1–12.

Gramsch E, Cereceda-Balic F, Oyola P *et al*., 2006. Examination of pollution trends in Santiago de Chile with cluster analysis of PM_{10} and ozone data. *Atmospheric Environment*, 40(28): 5464–5475.

Guo J P, Zhang X Y, Wu Y R *et al*., 2011. Spatio-temporal variation trends of satellite-based aerosol optical depth in China during 1980–2008. *Atmospheric Environment*, 45(37): 6802–6811.

Henderson S B, Beckerman B, Jerrett M *et al*., 2007. Application of land use regression to estimate long-term concentrations of traffic-related nitrogen oxides and fine particulate matter. *Environmental Science & Technology*, 41(7): 2422–2428.

Hoek G, Brunekreef B, Goldbohm S *et al*., 2002. Association between mortality and indicators of traffic-related air pollution in the Netherlands: A cohort study. *The Lancet*, 360(9341): 1203–1209.

Huang, Y, Yan Q, Zhang C, 2018. Spatial-temporal distribution characteristics of $PM_{2.5}$ in China in 2016, *Journal of Geovisualization and Spatial Analysis*, 2(2): 1–12.

Hueglin C, Gehrig R, Baltensperger U *et al*., 2005. Chemical characterisation of $PM_{2.5}$, PM_{10} and coarse particles at urban, near-city and rural sites in Switzerland. *Atmospheric Environment*, 39(4): 637–651.

Jiang Y A, Chen Y, Zhao Y Z *et al*., 2013. Analysis on changes of basic climatic elements and extreme events in Xinjiang, China during 1961–2010. *Advances in Climate Change Research*, 4(1): 20–29.

Kioumourtzoglou M A, Schwartz J, Weisskopf M *et al*., 2016. Long-term $PM_{2.5}$ exposure and neurological hospital admissions in the Northeastern United States. *Environmental Health Perspectives*, 124(1): 23–29.

Kloog I, Nordio F, Coull B *et al*., 2012. Incorporating local land use regression and satellite aerosol optical depth in a hybrid model of spatiotemporal $PM_{2.5}$ exposures in the Mid-Atlantic states. *Environmental Science & Technology*, 46(21): 11913–11921.

Laden F, Neas L M, Dockery D W *et al*., 2000. Association of fine particulate matter from different sources with daily mortality in six US cities. *Environmental Health Perspectives*, 108(10): 941–947.

Laden F, Schwartz J, Speizer F E *et al*., 2006. Reduction in fine particulate air pollution and mortality. *American Journal of Respiratory and Critical Care Medicine*, 173(6): 667–672.

Lindner A, Pitombo C S, 2018. A conjoint approach of spatial statistics and a traditional method for travel mode choice issues. *Journal of Geovisualization and Spatial Analysis*, 2(1): 1–13.

Lin G, Fu J, Jiang D *et al*., 2013. Spatio-temporal variation of $PM_{2.5}$ concentrations and their relationship with geographic and socioeconomic factors in China. *International Journal of Environmental Research and Public Health*, 11(1): 173–186.

Liu Y, Paciorek C J, Koutrakis P *et al*., 2009. Estimating regional spatial and temporal variability of $PM_{2.5}$ concentrations using satellite data, meteorology, and land use information. *Environmental Health Perspectives*, 117(6): 886–892.

Liu Y, Sarnat JA, Kilaru V *et al*., 2005. Estimating ground-level $PM_{2.5}$ in the eastern using satellite remote sensing. *Environmental Science & Technology*, 39(9): 3269–3278.

Liu Y S, Yang R, 2012. The spatial characteristics and formation mechanism of the county urbanization in China. *Acta Geographica Sinica*, 67(8): 1011–1020. (in Chinese)

Lu B, Kong S F, Han Bin, 2011. Inventory of atmospheric pollutants discharged from biomass burning in China continent in 2007. *China Environmental Science*, 31(2): 186–194. (in Chinese)

Merbitz H, Buttstädt M, Michael S *et al*., 2012. GIS-based identification of spatial variables enhancing heat and poor air quality in urban areas. *Applied Geography*, 2012, 33(4): 94–106.

Pope C A, 2000. Review: Epidemiological basis for particulate air pollution health standards. *Aerosol Science & Technology*, 32(1): 4–14.

Pope C A, Burnett R T, Thun M J *et al*., 2002. Lung cancer, cardiopulmonary mortality, and long-term exposure to fine particulate air pollution. *Jama*, 287(9): 1132–1141.

Pope C A, Dockery D W, Schwartz J, 1995. Review of epidemiological evidence of health effects of particulate air pollution. *Inhalation Toxicology*, 7(1): 1–18.

Samet J M, Dominici F, Curriero F C *et al*., 2000. Fine particulate air pollution and mortality in 20 U.S cities, 1987–1994. *New England Journal of Medicine*, 343:(24): 1742–1749.

Stone B, 2008. Urban sprawl and air quality in large US cities. *Journal of Environmental Management*, 86(4): 688–698.

Wang H, Dwyer-Lindgren L, Lofgren K T *et al*., 2012. Age specific and sex-specific mortality in 187 countries, 1970–2010: A systematic analysis for the global burden of disease study 2010. *The Lancet*, 380(9859): 2071–2094.

Wang J, Christopher S A, 2003. Intercomparison between satellite-derived aerosol optical thickness and $PM_{2.5}$ mass: Implications for air quality studies. *Geophysical Research Letters*, 30(21): 1–4.

Wang J F, Li X H, George Christakos *et al*., 2010. Geographical detectors-based health risk assessment and its application in the neural tube defects study of the Heshun Region, China. *International Journal of Geographical Information Science*, 24(1): 107–127.

Wang Z B, Fang C L, Xu G *et al*., 2015. Spatial-temporal characteristics of the $PM_{2.5}$ in China in 2014. *Acta Geographica Sinica*, 70(11): 1720–1734. (in Chinese)

Wu D, 2012. Hazy weather research in China in the last decade: A review. *Acta Scientiae Circumstantiae*, 32(2): 257–269.

Xu W, He F, Li H *et al*., 2014. Spatial and temporal variations of $PM_{2.5}$ in the Pearl River Delta. *Research of Environmental Sciences*, 27(9): 951–957.

Xue W, Wu W, Fu F *et al*., 2015. Satellite retrieval of a heavy pollution process in January 2013 in China. *Environmental Science*, 36, (3): 794–800. (in Chinese)

Xue W B, Fu F, Wang J N *et al*., 2014. Numerical study on the characteristics of regional transport of $PM_{2.5}$ in China. *China Environmental Science*, 34(6): 1361–1368. (in Chinese)

Yi H, Hao J, Tang X L *et al*., 2007. Atmospheric environmental protection in China: Current status, developmental. *Energy Policy*, 35(2): 907–915.

Zhang Y, Cao F, 2015. Fine particulate matter ($PM_{2.5}$) in China at a city level. *Scientific Reports*, 5: 1–11.

Zhang Y, Zhang W, Wang J *et al*., 2015. Establishment and application of pollutant inventory-chemical mass balance (I-CMB) model for source apportionment of $PM_{2.5}$. *Transactions of Atmospheric Sciences*, 38(2): 279–284. (in Chinese)